Available online at www.sciencedirect.com
SCIENCE DIRECT®
International Journal of Fatigue 25 (2003) 843–854
International Journal of Fatigue
www.elsevier.com/locate/ijfatigue

On the dominant role of crack closure on fatigue crack growth modeling

Marco Antonio Meggiolaro, Jaime Tupiassú Pinho de Castro *

Department of Mechanical Engineering, Pontifical Catholic University of Rio de Janeiro, Rua Marquês de São Vicente 225 Gávea, Rio de Janeiro, RJ, 22453-900, Brazil

Abstract

Crack closure is the most used mechanism to model thickness and load interaction effects on fatigue crack propagation. But assuming it is the only mechanism is equivalent to suppose that the rate of fatigue crack growth da/dN is primarily dependent on $\Delta K_{eff} = K_{max} - K_{op}$, not on ΔK. But this assumption would imply that the normal practice of using da/dN×ΔK curves measured under plane-stress conditions (without considering crack closure) to predict the fatigue life of components working under plane-strain could lead to highly *non*-conservative errors, because the expected fatigue life of "thin" (plane-stress dominated) structures could be much higher than the life of "thick" (plane-strain dominated) ones, when both work under the same stress intensity range and load ratio. However, crack closure cannot be used to explain the overload-induced retardation effects found in this work under plane-strain, where both crack arrest and delays were associated to an *increase* in ΔK_{eff}. These results indicate that the dominant role of crack closure in the modeling of fatigue crack growth should be reviewed.

Keywords: Fatigue crack growth; Crack closure; Sequence effects; Thickness effect

1. Introduction

It is well-known that load cycle interactions can have a very significant effect in fatigue crack growth (FCG) under variable amplitude (VA) loading. There is a vast literature proving that tensile overloads (OL), when applied over a baseline constant amplitude (CA) loading, can retard or even arrest a fatigue crack, and that compressive underloads (UL) can accelerate the subsequent FCG rate [1–7]. Neglecting these effects in fatigue calculations under VA loading can lead to completely invalid life predictions. In fact, when modeling many important real fatigue problems, only after considering overload-induced retardation effects can the actual life reached by some structural components be justified.

However, for design purposes it is particularly difficult to generate a universal algorithm to quantify these sequence effects on FCG, due to the number and to the complexity of the mechanisms involved in this problem, among them plasticity-induced crack closure, blunting and/or bifurcation of the crack tip, residual stresses and strains, strain-hardening, strain-induced phase transformation, crack face roughness, and oxidation of the crack faces, for example.

Besides, depending on the case, several of these mechanisms may act concomitantly or competitively, as a function of factors such as piece thickness (which controls the dominant stress-state at the crack tip), crack size, material microstructure, and environment. Moreover, the relative importance of these mechanisms can vary from case to case, and there is so far no universally accepted single equation capable of describing the whole problem. Therefore, from the fatigue designer's point of view, sequence and thickness effects must be treated in the most reasonably simplified way or, in Paris' words [1], FCG modeling must be kept simple.

But a simplified model must not be unrealistic, and so it is worthwhile mentioning that some simplistic models are unacceptable. For instance, it is not reasonable to justify the retardation effects by attributing to the overloads a significant variation in the residual stress-state at the crack tip. This is mechanically impossible, as the material around the crack tip yields in tension

* Corresponding author. Tel.: +55-21-2511-5846; fax: +55-21-3114-1165.
E-mail address: jtcastro@mec.puc-rio.br (J.T.P. Castro).

0142-1123/$ - see front matter © 2003 Elsevier Ltd. All rights reserved.
doi:10.1016/S0142-1123(03)00132-4

during the loading and in compression during the unloading of any propagating fatigue crack, forming the reversed plastic zone that always accompanies it. Therefore, there can be no significant variation in the residual stresses *at the crack tip* after an overload, where they already are of the order of the compressive yield strength of the material when the fatigue crack is unloaded.

On the other hand, the main characteristic of fatigue cracks is to propagate cutting a material that has already been deformed by the plastic zones that always accompany their tips. Therefore, fatigue crack faces are always embedded in an envelope of (plastic) residual strains and, consequently, they compress their faces when completely discharged, and open alleviating in a progressive way the (compressive) load transmitted through them, until reaching a load $P_{op} > 0$, after which the crack is completely opened, as discovered by Elber a long time ago [8].

Elber's plasticity-induced crack closure is the most popular load interaction mechanism. It has long been proved to satisfactorily explain plane-stress crack retardation effects [9]. In fact, neglecting crack closure in many fatigue life calculations can result in overly conservative predictions, increasing maintenance costs by unnecessarily reducing the period between inspections.

Even more important, according to some closure models, non-conservative predictions may arise from neglecting such effects. For instance, Newman [10–11] proposed that crack closure is not only a function of the load ratio $R = K_{min}/K_{max}$, where $K_{\min}$ and $K_{\max}$ are the minimum and the maximum values of the applied stress intensity factor (SIF) K, but it is also dependent on the stress-state and on the maximum stress level $\sigma_{\max}$. In this case, if plasticity-induced closure is the only mechanism affecting FCG, the life of "thin" structures (in which FCG is plane-stress dominated) can be expected to be much higher than the life of "thick" ones (where FCG occurs under plane-strain dominant conditions), when both work under the same stress intensity range ΔK and load ratio R. Therefore, if FCG $\mathrm{d}a/\mathrm{d}N \times \Delta K$ curves are measured under plane-stress conditions without considering crack closure, and then used to make life predictions on components which work under plane-strain, they could lead to *non*-conservative errors as high as 75% according to Newman's model, see Fig. 1. To avoid this error, it would be necessary to convert the measured crack growth constants associated with a given stress condition to the other using appropriate crack closure functions.

But such an important thickness effect is not recognized by the ASTM E645 standard on the measurement of FCG rates. In spite of mentioning the importance of crack closure, this standard only requires specimens sufficiently thick to avoid buckling during the tests, and correlates the FCG rate $\mathrm{d}a/\mathrm{d}N$ with ΔK, not with the effective range $\Delta K_{eff} = K_{max} - K_{op}$, as it should if crack closure would control all FCG problems. Moreover, if it is ΔK_{eff} and not ΔK that controls FCG, it would be necessary to calculate K_{op} along the crack path in order to predict the fatigue life, a task yet to be satisfactorily solved for most practical geometries.

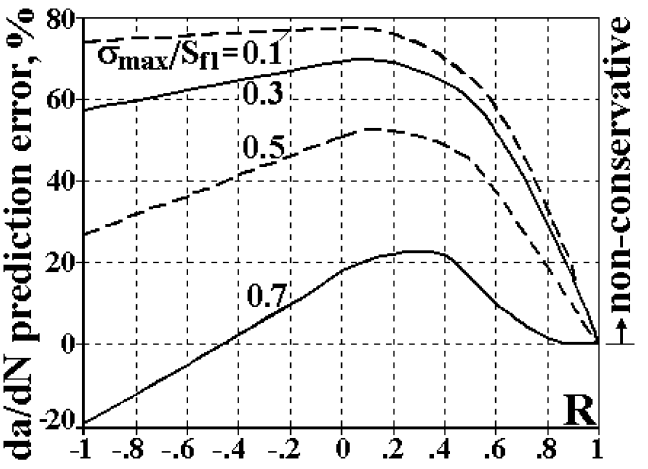

Fig. 1. Effect of the maximum stress $\sigma_{\max}$ and load ratio R on $\mathrm{d}a/\mathrm{d}N$ prediction errors for plane-strain calculations based on plane-stress data, according to Newman's closure function (Paris exponent 3.25).

However, it is not reasonable to assume that ΔK_{eff} controls all FCG problems. In this work, experiments on overload-induced retardation were performed under plane-strain conditions, however the measured delay cycles simply could not be explained by crack closure.

2. Plasticity-induced crack closure

Crack closure can be easily observed by measuring the load P applied on a cracked body and its associated load point displacement x (or the corresponding crack mouth displacement δ or the strain ε in any conveniently located body point, e.g., the back face strain in compact tension C(T) specimens, provided linear elastic fracture mechanics (LEFM) conditions are maintained during the test), as shown in Fig. 2. It is worth mentioning that in fatigue tests it is normally almost impossible to directly measure x, and that ε usually gives a cleaner signal than δ.

Crack closure is identified by the initial non-linear part of the P vs. x plot, indicating a progressive apparent decrease in the cracked body stiffness as the load is increased from zero, until the so-called opening load P_{op} is reached, above which the P vs. x graph remains linear (under LEFM conditions). Moreover, in this case the compliance $C(a_0) = x/P$ of a (plane) cracked body of thickness t and crack size a_0 can be correlated to its strain energy release rate $(P^2/2t)\cdot(\mathrm{d}C/\mathrm{d}a) = K_I)^2/E'$ [7]:

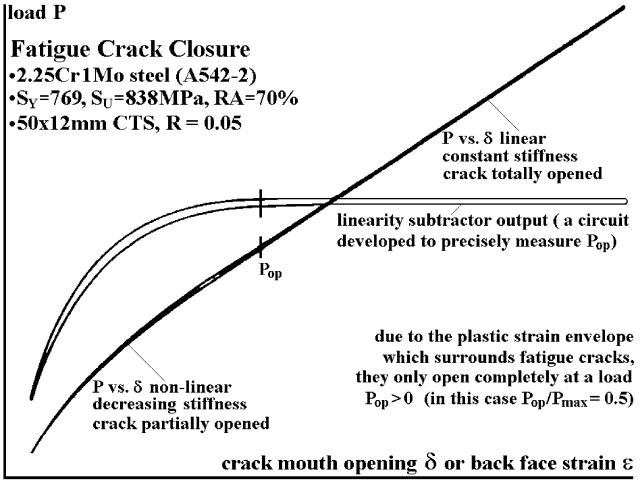

Fig. 2. Typical crack closure measurement, including a linearity subtractor to enhance the non-linear part of the $P \times \delta$ (or $P \times \varepsilon$) plot to precisely identify the opening load P_{op}.

$$\frac{dC}{da} = \frac{2tK_I^2}{P^2E'} = \frac{2t\sigma^2\pi}{P^2E'}\cdot[a\cdot f^2(a/w)] \therefore$$
$$C(a_0) = \frac{2t\sigma^2\pi}{P^2E'}\int_0^{a_0}[a\cdot f^2(a/w)]da + C(0) \quad (1)$$

where $C(0) = C(a_0 = 0)$ is the uncracked body compliance, $K_I = \sigma\sqrt{(\pi a)} \times f(a/w)$ is the mode I SIF, σ is the applied stress, a is the crack size, w is the body width (or other characteristic dimension), and E' is Young's Modulus, with $E' = E$ under plane-stress conditions or $E' = E/(1-\nu^2)$ under plane-strain, ν being Poisson's ratio.

Fig. 2 shows an example of a particularly precise P_{op} measurement during a fatigue crack propagation test. P_{op} must be measured at the very starting point of the linear part of the $P \times \delta$ (or $P \times \varepsilon$) curve, a task which can be easier achieved with the aid of a special circuit called the linearity subtractor [12] to enhance the non-linear initial part of the curve. It is important to point out that, in the authors' opinion, closure measurements based on global parameters like δ or ε are much more representative of the whole cracked body behavior than the local (or near crack tip) ones. These, being made on the body's surface, reflect its plane-stress behavior, which is not the dominant stress-state when FCG occurs in thick bodies.

In fact, the different behaviors caused by these surface effects have been verified from constant amplitude tests on center-cracked 10.2 mm thick 2024-T3 aluminum plate specimens [13]. In these tests, a crack opening stress of 28% of the maximum stress σ_{max} was found under a stress ratio $R = 0.1$. The specimens were then made thinner by removing surface layers at both sides of the plate specimens. After a thickness reduction to 7.7 mm, the crack opening stress dropped to 13% of σ_{max}, and after a further thickness reduction to 3.75 mm the result was 11% of σ_{max}. Because the major change in the opening stress was caused by the first thickness reduction, it is suggested that crack closure occurs predominantly near the material surface, under plane-stress conditions.

Similar tests were performed by McEvily [14], using 6061-T6 aluminum compact specimens. In these tests, a typical crack growth retardation behavior was found after a 100% overload due to the developed crack closure, however when both specimen surfaces were machined away (reducing its thickness to half its original value) the retardation effect was largely eliminated.

More crack closure near the surface agrees with the expected larger plastic zone sizes for plane-stress than for plane-strain. Paris and Hermann [15] suggested that fatigue cracks open first at mid-thickness and later at the material surface, therefore crack closure would be in fact a 3D phenomenon. As a result of more crack closure at the material surface, the crack front lags behind where it intersects the material surface, leading to curved crack fronts for through-cracks in very thick specimens. Experiments on a 75 mm thick steel specimen under constant amplitude loading showed a crack front curvature with a lagging of 6.8 mm at the surface if compared to its mid-thickness plane-strain front [16]. However, such lagging is hardly observed in thinner specimens.

It might be stated that crack closure is predominantly a surface phenomenon occurring under plane-stress conditions. Since plastic deformations do not result in volume change, any plastic elongation in the loading direction must be compensated by a negative plastic strain in the thickness direction, which indeed occurs at the material surface. However, under pure plane-strain conditions, the strain in the thickness direction is zero, making it impossible to develop residual tensile strains at the crack faces, unless compressive plastic strains were to be found in the crack growth direction, which is not observed in practice [17].

To quantify the effects of crack closure, Elber [8] attempted to describe, with the aid of a physical model, the connection between load sequence, plastic deformation (by way of crack closure), and crack growth rate. As mentioned above, he assumed that crack extension could not take place under cyclic loads until it was fully opened, because only when $P_{op} > 0$ would the crack tip be stressed. Therefore, the bigger P_{op} and the corresponding K_{op}, the less would be the effective stress intensity range $\Delta K_{eff} = K_{max} - K_{op}$, and this ΔK_{eff} instead of $\Delta K = K_{max} - K_{min}$ would be the fatigue crack propagation controlling parameter. Based on experiments on 2024-T3 aluminum, Elber proposed a modification to the Paris growth equation taking into account the crack closure concept:

$$\frac{da}{dN} = A\cdot(K_{max} - K_{op})^m = A\cdot(\Delta K_{eff})^m \quad (2)$$

where A and m are material constants, which should be experimentally measured.

Since $\Delta K = K_{max} - K_{min}$ and $R = K_{min}/K_{max}$, then the stress intensity range can be rewritten as $\Delta K = (1-R) \times K_{max}$. Therefore, since the crack stops below the FCG threshold (i.e., $da/dN \to 0$ when $\Delta K \to \Delta K_{th}$) and assuming that crack arrest is only due to Elber's closure (where the crack stops if $K_{max} \leq K_{op}$), then ΔK_{th} should depend on R through $\Delta K_{th} = (1-R) \times K_{op}$, and thus

$$\frac{da}{dN} = A\cdot(\Delta K_{eff})^m = A\cdot\left(\frac{(K_{max}-K_{op})\cdot(1-R)}{1-R}\right)^m = A\cdot\left(\frac{\Delta K-\Delta K_{th}}{1-R}\right)^m \quad (3)$$

This equation assumes $R > 0$. Walker and Chang [18] proposed a similar FCG equation considering the effects of negative R ratios, but their original formulation did not include explicitly the effect of ΔK_{th}, so in this paper a modified version is proposed, as follows.

For $\Delta K > \Delta K_{th}$ and $R \geq 0$,

$$\frac{da}{dN} = A\cdot\frac{(\Delta K-\Delta K_{th})^m}{(1-\bar{R})^p}, \text{ where } \bar{R} = \begin{cases} R, & \text{if } R < R^+ \\ R^+, & \text{if } R \geq R^+ \end{cases} \quad (4)$$

for $\Delta K > \Delta K_{th}$ and $R < 0$,

$$\frac{da}{dN} = A\cdot(K_{max}-\Delta K_{th})^m(1+\bar{R}^2)^q, \text{ where } \bar{R} = \begin{cases} R, & \text{if } R > R^- \\ R^-, & \text{if } R \leq R^- \end{cases} \quad (5)$$

and for $\Delta K \leq \Delta K_{th}$,

$$da/dN = 0 \quad (6)$$

where A, m, p and q are experimentally measured constants, and R^+ and R^- are the cutoff values for positive and negative stress ratios. Walker and Chang used $R^+ = 0.75$ and $R^- = -0.5$ for the above equations. Note that the constant q must be determined from test data generated for specific negative stress ratios ($R < 0$). The threshold stress intensity factor range used in these FCG models can be determined for any positive stress ratio $R > 0$ by an empirical equation:

$$\Delta K_{th} = (1-\alpha_t R)\Delta K_0 \quad (7)$$

where ΔK_0 is the crack propagation threshold obtained from $R = 0$ CA tests, and α_t is a constant determined from CA test data obtained under various stress ratios. Another expression for the variation of ΔK_{th} as a function of R ($R > 0$) was proposed by Forman and Mettu [19]:

$$\Delta K_{th} = (4/\pi)\cdot\Delta K_0\cdot\arctan(1-R) \quad (8)$$

However, Newman et al. [10,11] concluded from Finite Element calculations that crack closure does not depend only on R, as proposed by Elber, but it is also dependent on the maximum stress level σ_{max}. They proposed a crack opening function f, defined as the ratio K_{op}/K_{max} between the crack opening and the maximum stress intensity factor at each cycle. This function depends on R and also on the ratio between the maximum stress σ_{max} and the material flow strength S_{fl} (for convenience defined as the average between the material yielding and ultimate strengths, $S_{fl} = (S_Y + S_U)/2$), and on a plane stress/strain constraint factor α, ranging from $\alpha = 1$ for pure plane-stress to $\alpha = 1/(1-2\nu)$ for pure plane-strain, where ν is Poisson's ratio:

$$f = \frac{K_{op}}{K_{max}} = \begin{cases} \max(R, A_0 + A_1 R + A_2 R^2 + A_3 R^3), R \geq 0 \\ A_0 + A_1 R, -2 \leq R < 0 \end{cases} \quad (9)$$

where the polynomial coefficients are given by:

$$\begin{cases} A_0 = (0.825-0.34\alpha+0.05\alpha^2)\cdot[\cos(\pi\sigma_{max}/2S_{fl})]^{1/\alpha} \\ A_1 = (0.415-0.071\alpha)\cdot\sigma_{max}/S_{fl} \\ A_2 = 1-A_0-A_1-A_3 \\ A_3 = 2A_0 + A_1 - 1 \end{cases} \quad (10)$$

From the definition of Newman's closure function f, the effective stress intensity range ΔK_{eff} can be rewritten as

$$\Delta K_{eff} = (1-f)\cdot K_{max} = \frac{1-f}{1-R}\Delta K \quad (11)$$

Substituting Eqs. (9) and (10) into (11), correlations between ΔK_{eff} and the stress ratio R can be obtained for the plane-stress ($\alpha = 1$) and plane-strain ($\alpha = 3$) conditions, assuming $\nu = 0.33$ and $\sigma_{max}/S_{fl} = 0.3$ which, according to [11], would be a mean value for typical specimens used in FCG tests:

$$\frac{\Delta K_{eff}}{\Delta K} = \begin{cases} 0.52 + 0.42R + 0.06R^2, R \geq 0 \text{ (plane stress)} \\ (0.52-0.1R)/(1-R), \ -2 \leq R < 0 \text{ (plane stress)} \\ \min(1, \ 0.75 + 0.69R - 0.44R^2), R \geq 0 \text{ (plane strain)} \\ (0.75-0.06R)/(1-R), \ -2 \leq R < 0 \text{ (plane strain)} \end{cases} \quad (12)$$

Another correlation between ΔK_{eff} and R was obtained by Schijve [20],

$$\Delta K_{eff} = \Delta K(0.55 + 0.35R + 0.1R^2) \quad (13)$$

Schijve's equation is also based on the fatigue crack closure concept, agreeing within 7% with Newman's predictions for the plane-stress case. Moreover, if α is

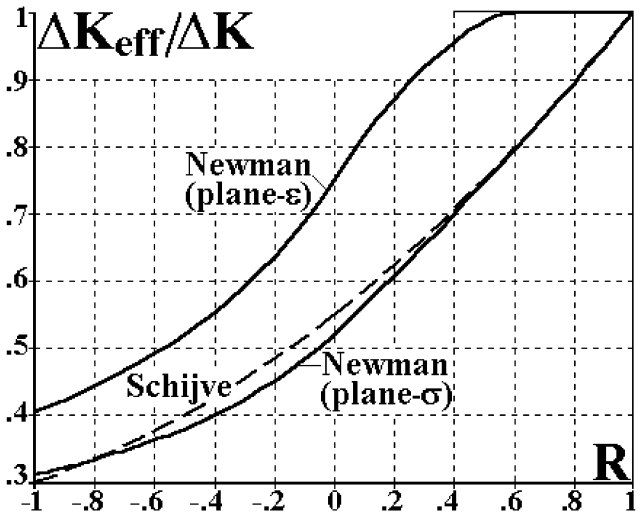

Fig. 3. Effective stress intensity ΔK_{eff} ranges as a function of the stress ratio R.

interpreted as a curve-fitting parameter, then a value $\alpha = 1.15$ would have a better agreement with Schijve's correlation, instead of assuming $\alpha = 1$. In practice, this is a sound idea because many specimens under pure plane-strain conditions according to ASTM E399 (which validates K_{IC} toughness tests) have in fact constraint factors α between 1.9 and 2.7, instead of the theoretical value $\alpha = 3$ [11].

Fig. 3 compares Eqs. (12) and (13) as a function of R. Note that the predicted closure effects are much smaller under plane-strain than under plane-stress conditions, and that Newman's closure function predicts no crack closure (and therefore $\Delta K_{eff}/\Delta K = 1$) under dominantly plane-strain conditions for stress ratios R roughly above 0.5.

In addition, increasing $\sigma_{\max}$ reduces Newman's closure function, resulting in predictions of higher da/dN rates. Figs. 4 and 5 compare effective stress intensity

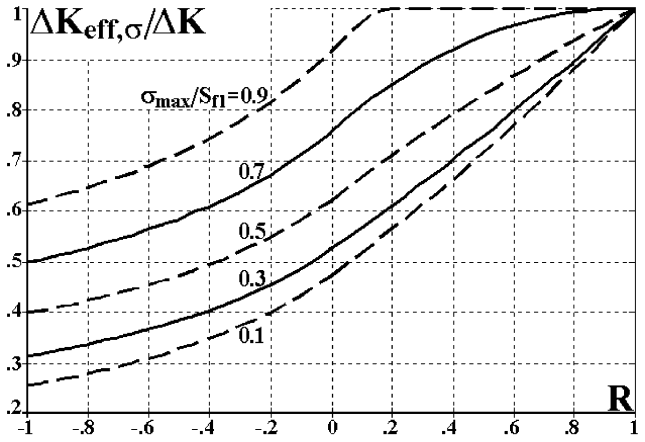

Fig. 4. Effect of $\sigma_{\max}$ on Newman's effective stress intensity range $\Delta K_{\text{eff},\sigma}$ under plane-stress.

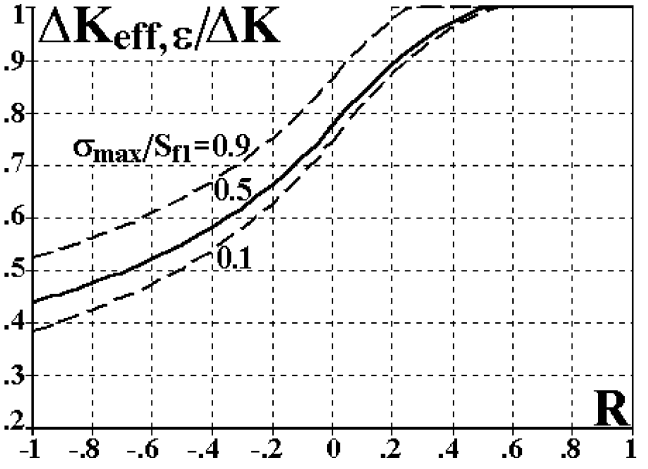

Fig. 5. Effect of $\sigma_{\max}$ on Newman's effective stress intensity range $\Delta K_{\text{eff},\varepsilon}$ under plane-strain.

ranges predicted by Newman for plane-stress, $\Delta K_{\text{eff},\sigma}$, and for plane-strain, $\Delta K_{\text{eff},\varepsilon}$, under different stress levels $\sigma_{\max}/S_{\text{fl}}$. Fig. 6 shows that Newman's effective stress intensity ranges can assume very different values for plane-stress and for plane-strain, especially when $\sigma_{\max}/S_{\text{fl}}$ is low.

Based on the above expressions for the effective stress intensity range, Forman and Newman proposed the following fatigue crack propagation equation to model all three crack growth regimens, including the effect of the stress-state through Newman's closure function [19]:

$$\frac{\mathrm{d}a}{\mathrm{d}N} = A\cdot\left(\frac{1-f}{1-R}\Delta K\right)^{m}\cdot\left(1-\frac{\Delta K_{\text{th}}}{\Delta K}\right)^{p}\Big/\left(1-\frac{K_{\max}}{K_C}\right)^{q} \qquad (14)$$

where K_C is the critical (rupture) stress intensity factor, and A, m, p, and q are experimentally adjustable constants.

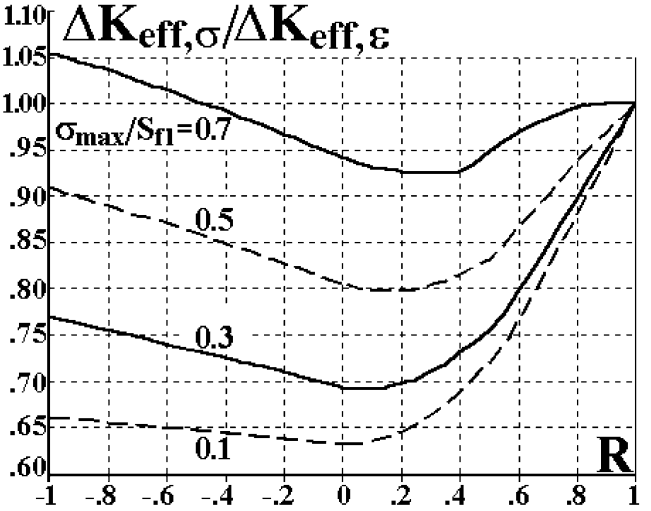

Fig. 6. Effect of $\sigma_{\max}$ and R on the ratio between Newman's effective stress intensity ranges under plane-stress and plane-strain, $\Delta K_{\text{eff},\sigma}/\Delta K_{\text{eff},\varepsilon}$.

Assuming that the fatigue crack growth rate is controlled by ΔK_{eff} instead of ΔK (and, therefore, that plasticity induced closure is the sole mechanism which affects the propagation process), then the need for taking into account the stress-state effect in fatigue crack propagation tests must be emphasized. Consider, for instance, the effective stress intensity range ΔK_{eff} predicted by Newman for the plane-stress case when $R = 0$. In this case, according to Fig. 3, ΔK_{eff} is approximately equal to half the value of ΔK. This means that da/dN curves experimentally fitted to ΔK values without considering the crack closure effect would be actually correlating the measured da/dN rates with twice the actual (effective) stress intensity range acting on the crack tip. On the other hand, da/dN curves obtained in the same way ($R = 0$) under plane-strain conditions would be actually correlating da/dN with 4/3 of (and not twice) the effective stress intensity range. Therefore, one could not indiscriminately use crack growth equation constants obtained under a certain stress condition (e.g. plane-stress) to predict crack growth under a different state (e.g. plane-strain), even under the same stress ratio R.

Also, if a Paris da/dN vs. ΔK equation with exponent $m = 3.0$ (measured under plane-stress conditions and $R = 0$) is used to predict crack propagation under plane-strain, the predicted crack growth rate would be $[(4/3)/2]^m \approx 0.3$ times the actual rate, a *non*-conservative error of 70%. Therefore, to avoid this (unacceptable) error, it would be necessary to convert the measured crack growth constants associated with one stress condition to the other using appropriate crack closure functions. Another approach would be to use in the predictions only da/dN vs. ΔK equations such as Eq. (14), which has already embedded the stress-state dependent closure functions.

This alarming prediction implies that the usual practice of plotting da/dN vs. ΔK instead of da/dN vs. ΔK_{eff} to describe fatigue crack growth tests would be highly inappropriate, because da/dN would also be a strong function of the specimen thickness t, which controls the dominant stress-state at the crack tip. Also, assuming that the classical ASTM E399 requirements for validating a K_{IC} toughness test could also be used in fatigue crack growth, plane-strain conditions would only apply if $t > 2.5(K_{max}/S_Y)^2$. In other words, one could expect to measure quite different da/dN fatigue crack growth rates when testing thin or thick specimens of a given material under the same ΔK and R conditions. Moreover, the concept of a "thin" or "thick" specimen would also depend on the load, since $K_{\max}$ increases with the applied stress. However, this thickness effect on da/dN is not recognized by the ASTM E645 standard on the measurement of fatigue crack propagation, which, in spite of mentioning the importance of crack closure, only requires specimens sufficiently thick to avoid buckling during the tests.

The errors associated with plotting da/dN vs. ΔK instead of ΔK_{eff} to predict crack growth under different stress states can be illustrated, e.g., using $m = 3.25$ for the exponent of the Paris equation of an aluminum alloy. If data is measured under plane-stress conditions without considering crack closure, then the prediction under plane strain would be $(\Delta K_{\text{eff},\sigma}/\Delta K_{\text{eff},\varepsilon})^m$ times the actual rate, a non-conservative error of $[1-\Delta K_{eff,\sigma}/\Delta K_{eff,})^{3.25}]$. Using the ratio $\Delta K_{\text{eff},\sigma}/\Delta K_{\text{eff},\varepsilon}$ calculated from Newman's closure function (Fig. 6), this prediction error is plotted in Fig. 1 as a function of $\sigma_{\max}$ and R.

In summary, since it is the thickness t the parameter that controls the dominant stress-state in FCG, one could expect the fatigue life of thin sheets (associated with larger plastic zones) to be much higher than the life of thick plates (with smaller plastic zones), when both work under the same (initial) $\Delta \boldsymbol{K}$ and R. One could also expect intermediate thickness structures, where the stress-state is not plane-stress nor plane-strain dominated, to have $1 < \alpha < 1/(1-2\nu)$ and a transitional behavior. Moreover, this transition can occur in the same specimen if the crack starts under plane-strain and progressively grows toward a plane-stress dominated state. However, unlike the thickness effect on fracture toughness, the dominant stress-state usually is not object of much concern in fatigue design, but it certainly deserves a closer experimental verification.

On the other hand, it must be pointed out that many of the above results were derived from Finite Element calculations, and not from experimental measurements [10–11,21]. It is a known fact that elastic–plastic FE calculations may offer significant problems due to non-linear aspects including material plasticity as well as changing contacts between the fracture surfaces during crack closure and opening [17]. In addition, the question whether plane-strain or plane-stress is applicable in the FE calculations is another problematic issue, essential to calculate the plastic zone sizes and therefore the plastic wake field of a crack.

Also, the FE models presented above assume that crack closure occurs everywhere near (and behind) the crack tip, including at the crack tip itself. However, Paris et al. [1] suggested that crack closure only occurs beyond a small distance d behind the crack tip, a phenomenon termed partial closure. Therefore, in an unloaded cracked body, the plastic strain wake around the crack faces would work as a wedge of thickness $2h$ that would cause a non-zero stress intensity of

$$K_{\text{eff}_{\min}} = E' h / \sqrt{2\pi d} \tag{15}$$

To completely open the crack, releasing all compressive loads over the wedge, the crack opening displacement COD at a distance d of the crack tip must be equal to $2h$, therefore

$$\text{COD} = \frac{4K_{\text{op}}}{E'}\sqrt{\frac{2d}{\pi}} = 2h \Rightarrow$$
$$K_{\text{eff}_{\min}} = \frac{E'}{\sqrt{2\pi d}}\frac{2K_{\text{op}}}{E'}\sqrt{\frac{2d}{\pi}} = \frac{2}{\pi}K_{\text{op}} \quad (16)$$

It is interesting to point out that $K_{\text{eff}_{\min}}$ does not depend on d or on $2h$. Therefore, from Eq. (16) it can be concluded that

$$\Delta K_{\text{eff}} = K_{\max} - (2/\pi)K_{\text{op}} \quad (17)$$

would be the actual effective stress range under plasticity-induced crack closure conditions. This equation assumes that $K_{min} \leq 0$, but if $0 < K_{min} \leq K_{op}$, then

$$K_{\max} - (2/\pi)K_{\text{op}} - (1-2/\pi)K_{\min} \leq \Delta K_{\text{eff}} \leq K_{\max} - (2/\pi)K_{\text{op}} \quad (18)$$

This ΔK_{eff} fitted well phase I of the FCG curve of aluminum alloys, but its performance on phase II was a little bit disperse [1]. A better fitting was obtained substituting the constant $2/\pi$ by an adjustable parameter p, which varies from $p = 2/\pi$ close to ΔK_{th} until $p = 1$ in the Paris regime [22]. The partial closure model presented above shows the original crack closure concept in a somewhat different light, yet maintaining its important role in FCG modeling.

But a closer survey of the literature reveals a series of test results that might even contradict some of the basic crack closure assumptions. When examining Ti-6Al-4V by the electropotential method, Shih and Wei [23] confirmed that crack closure depends on R and on $K_{\max}$, which is in agreement with Dugdale's theory [24]. However, in that titanium alloy no crack closure was found for $R > 0.3$. According to Shih and Wei, neither the influence of R on the crack propagation nor the retardation effects could be completely explained by crack closure.

Bachmann and Munz [25] also conducted crack closure measurements on Ti-6Al-4V, using an extensometer. However, unlike Shih and Wei, they were not able to discover any influence of $K_{\max}$ on crack closure behavior.

Kim and Shim [26] found that the variance of da/dN is increased in thin specimens of 7075-T6 aluminum alloy, but no significant thickness dependence of the average da/dN rates was reported.

Other conflicting results have been found in the literature for tests under constant amplitude loading. Compact tension C(T) specimens of 304 stainless steel with thicknesses varying between 3 and 25 mm tested under CA loads showed a relatively small thickness dependence [27]. It was found that the crack propagation rate on the 3 mm specimen was 30% smaller than on the 25 mm one, which is not much beyond the regular scatter of the experimental data. Costa and Ferreira [28] measured the growth rates on C(T) specimens of CK45 steel, with thicknesses varying between 6 and 24 mm. It was found that the thickness dependence was only significant for low R ratios ($R<0.2$) and low ΔK levels, while at $R = 0.4$ no thickness effect could be observed. Such results might be explained either by different production techniques used to obtain the considered thicknesses (which could lead to different microstructures and therefore affect the growth rates), or simply by the fact that plasticity-induced closure may not be the main retardation mechanism in many cases, especially under higher R ratios.

On the other hand, tests under variable amplitude loading show a more systematic trend of increased retardation in thinner specimens. FCG retardation following an overload is usually dependent on the plastic zone size, which can be explained considering either crack closure or residual stress mechanisms. Thus, it should be expected that retardation effects are more intense in thinner specimens, which present larger plastic zones, as confirmed by tests performed by Mills and Hertzberg [29] on 2024-T3 aluminum specimens. It is also found that higher OL levels result in increased retardation, which can be explained by a larger OL plastic zone.

A marked thickness effect under VA loading has also been found in tests performed by Saff and Holloway [30] on center-cracked specimens under a load spectrum based on F-4 aircraft loads. In these tests, the fatigue life of thick plates was found to be about 10 times shorter than for thin sheets. Results from Schijve [31] and Bernard et al. [16] showed the same trend.

Shuter and Geary [32–33] performed single overload tests on C(T) specimens made of BS 4360 Gr.50D carbon-manganese steels, with thicknesses in the range 5–25 mm. They suggested that there is a linear relationship between specimen thickness and the logarithm of the delay cycles. Also, crack retardation was found at baseline R-ratios as high as 0.5, even though no crack closure was detected at this R value. It is an obvious conclusion of this observation that if there is no crack closure, this mechanism simply cannot explain the crack retardation effects measured at that high R ratio.

It has been suggested [3] that the plasticity induced crack closure mechanisms do operate at such high R ratios, however closure cannot be measured because the dimensional changes at the crack tip are too small to be detected by the mechanical compliance method. However, this argument is difficult to accept because compliance measurements are used in the first place to prove that crack closure exists and, more important, to obtain the *precise* opening load, which is essential to obtain ΔK_{eff} and to check its influence in fatigue life predictions.

In opposition, Lang and Marci [5] claim that crack closure following an overload does not occur at high R values such as 0.5, and therefore crack closure can only

play a secondary role. They attribute the retardation phenomenon primarily to the residual compressive stresses ahead of the crack tip after an overload.

Another possible explanation could be due to crack path deflections or bifurcations [34–35], which can cause retardation even under high *R*-ratios due to the reduction in the stress intensity factor values caused by crack kinking or branching. However, since crack bifurcation has not been subject of much work in the literature, it is now being extensively studied with the aid of a specialized Finite Element program called Quebra2D and a general purpose fatigue software named ViDa [36,38,39].

3. Experimental results

A comprehensive study on single overload effects in plane-strain fatigue crack growth was made using 50 × 12.8 mm C(T) specimens of a tempered martensitic ASTM A-542/2 (2.25Cr1Mo) steel with yield strength S_Y = 769 MPA, ultimate strength S_U = 38 MPa, hardness *23HRc*, and reduction in area *RA* = 70%. Plane-strain conditions were enforced trying to maintain the OL plastic zone size much smaller than the specimen thickness *t*, or $zp_{OL} << t$ = 12.8 mm, where the symbol "<<" was arbitrarily chosen in the ASTM E-399 standard sense. Indeed, in most experiments $t >> 2.5(K_{max}/S_Y)^2$, where K_{max} is the stress intensity factor associated to the OL peak.

The FCG tests were performed at two *R* ratios, *R* = 0.05 and *R* = 0.7. The crack length was measured using a precise DC potential drop system, which had an uncertainty of 20 μm [37]. The measured FCG curves of the A-542/2 steel at these two *R* ratios are shown in Fig. 7. Both Δ*K* increasing and Δ*K* decreasing data are shown in that figure. The 50 Hz sinusoidal loads were applied under load control in a servo-hydraulic testing machine.

All *R* = 0.05 OL tests were made at a baseline (BL) stress intensity factor ΔK_{BL} = 10 MPa√m, a point slightly above the transition from phase I to phase II FCG. OL tests at *R* = 0.7 were made at ΔK_{BL} = 8 or ΔK_{BL} = 10 MPa√m, to obtain BL FCG conditions similar to the *R* = 0.05 tests.

The (single) OL were slowly applied after stopping the test machine at the minimum BL load, in order to keep the process under close control. Special care was taken to avoid overshooting when restarting ΔK_{BL} after completing the overload routine. Several OL were applied in a same specimen, but always only after the effect of the previous one was completely overcome. This was assured by letting the BL FCG rate be regained and then maintained during a crack increment several times larger than the plastic zone size zp_{OL} of the previous OL.

As 200% was the maximum value of the OL applied in the *R* = 0.05 tests, in all these low *R* cases $zp_{OL} <$ 270 μm (assuming that $zp_{OL} = (1/2\pi)(K_{max}/S_Y)^2$), which indeed was much smaller than the specimen thickness, justifying the plane-strain controlled FCG claim. In the *R* = 0.7 tests, the maximum OL was 100%, and the corresponding zp_{OL} = 1.2 mm, a little larger than the E-399 requirement but still an order of magnitude below the C(T) thickness.

An OL could have no detectable effect on the subsequent FCG rate, could delay the crack or even stop it, depending on its magnitude. Typical retardation results at *R* = 0.05 and *R* = 0.7 are shown in Figs. 8–11. Note that some curves in Figs. 8–11 are associated with negative cycles because the OL cycle was offset and defined as cycle number zero. Overloads of 25% (or a 1.25 ratio between the OL and the BL peaks) have no detectable effects under both *R* ratios, while 100% OL at *R* = 0.7 or 150% OL at *R* = 0.05 always stopped the cracks. Also, increasing retardation was observed between these 100% and 150% values (a crack arrest after a 134% OL at *R* = 0.05 is shown in Fig. 10). The overall crack behavior in the OL affected zone was similar but not identical to the classical plane-stress one, since no delayed retar-

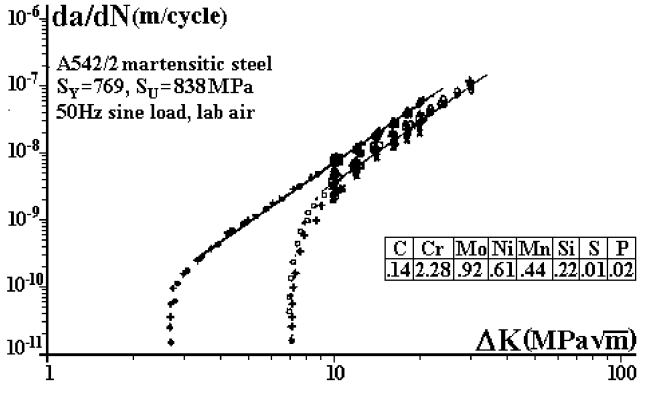

Fig. 7. A-542/2 steel d*a*/d*N* × Δ*K* FCG curves at *R* = 0.05 and *R* = 0.7.

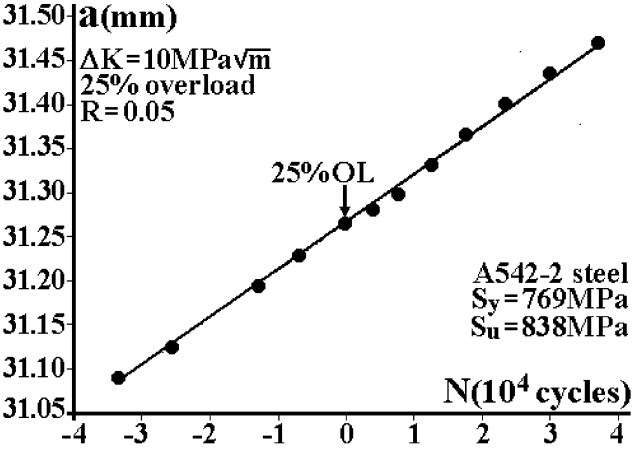

Fig. 8. No detectable crack retardation after a 25% overload, *R* = 0.05.

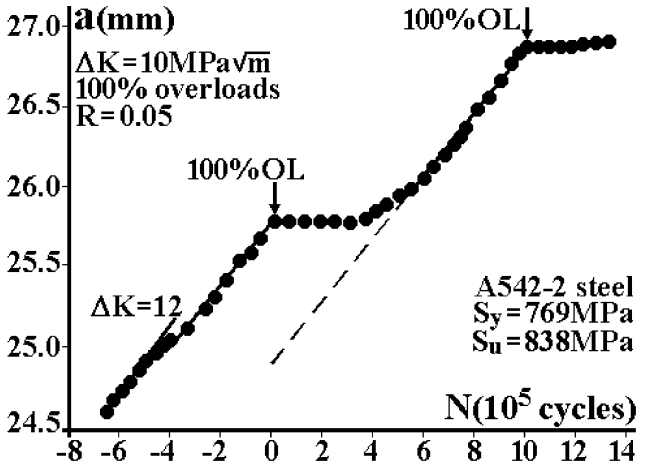

Fig. 9. Fatigue crack growth retardation after a 100% overload, $R = 0.05$.

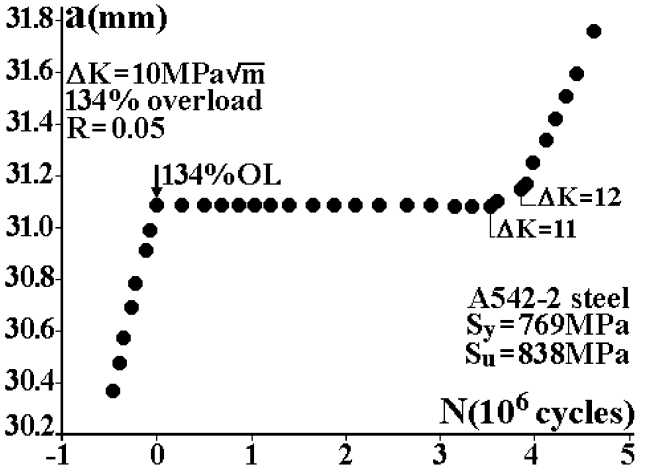

Fig. 10. Fatigue crack arrest after a 134% overload, $R = 0.05$.

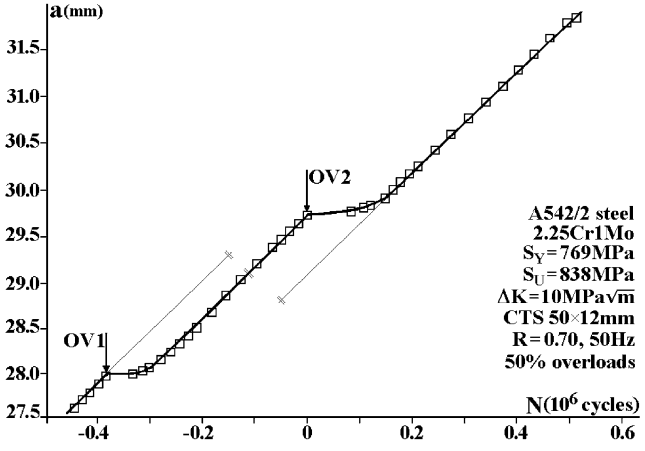

Fig. 11. Fatigue crack growth retardation after a 50% overload, $R = 0.7$.

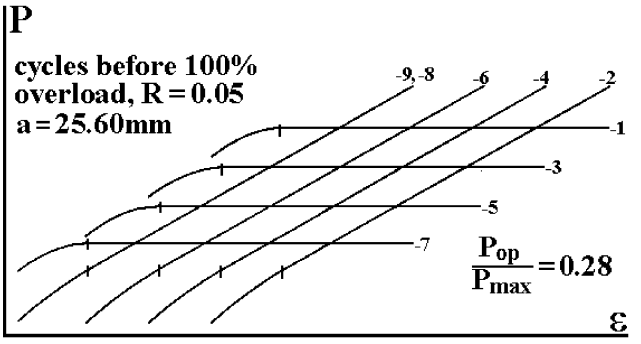

Fig. 12. Crack closure measurements before a 100% overload, $R = 0.05$. The OL cycle is arbitrarily called cycle 0, thus cycles before the OL are negative. Both $P \times \varepsilon$ and the correspondent linearity subtractor (LS) output curves are shown. The various coincident curves have been shifted for clarity.

dation was ever observed, and the size of the OL affected zone was generally smaller than zp_{OL}.

Careful crack closure measurements were made before and after the overloads, in order to study its influence on the subsequent FCG behavior. These measurements were particularly precise, and their scatter in consecutive cycles was negligible, as illustrated in Fig. 12. This figure shows several $P \times \varepsilon$ and $(P-k\varepsilon) \times \varepsilon$ curves measured in subsequent load cycles. This last type of curve is the linearity subtractor output, were k is the slope of the linear part of the $P \times \varepsilon$ curve, which was fitted by means of an analog differentiator, as described in [12]. The crack opening load P_{op} could then be easily identified, and a two-digit resolution on P_{op}/P_{max} measurements could be guaranteed. It must be pointed out that the various curves in Fig. 12 had to be displaced for clarity, otherwise they would be coincident. In all these measurements, $P_{op}/P_{max} = 0.28$.

Fig. 13 shows the closure measurements made just after the 100% OL was applied. Two very important features are evident from this figure. First, as in Fig. 12, the measurements are again very repeatable. Second, and

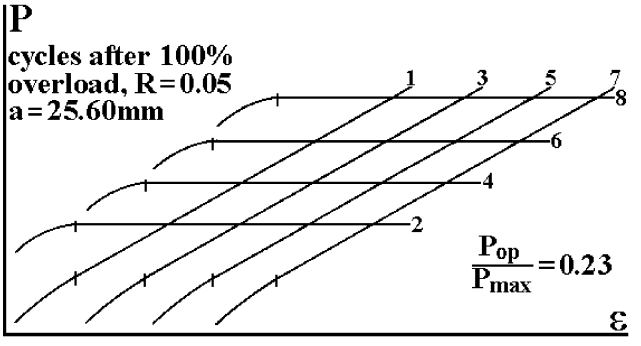

Fig. 13. Crack closure measurements just after the 100% OL reported in Fig. 12 show a *decrease* in the opening load P_{op}. The various coincident $P \times \varepsilon$ and LS curves measured in subsequent cycles have been shifted for clarity.

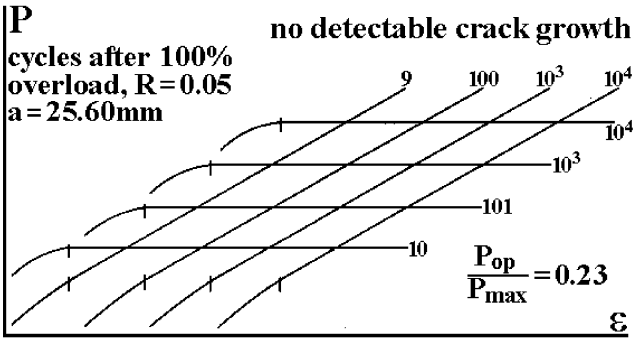

Fig. 14. Crack closure measurements in up to 10^4 cycles after the 100% OL reported in Fig. 12. During these measurements there was no detectable crack growth, despite the 22% *increase* in ΔK_{eff}. The various coincident curves have been shifted for clarity.

much more important, the crack opening load *decreased* after the OL, since $P_{op}/P_{max} = 0.23$ in this case. However, associated to this increase in ΔK_{eff}, no crack growth could be detected, and all P_{op} measurements in this period gave the same $P_{op}/P_{max} = 0.23$ result, as shown in Fig. 14. Only after 7.5×10^4 cycles could the potential drop system sense a small growth in the crack size, and this crack increment was associated to an *increase* in P_{op}, which rose to $P_{op}/P_{max} = 0.25$. Moreover, when the OL effect completely ceased, P_{op} returned to the value it had before the OL, see Fig. 15. This result, of course, is exactly the opposite of what would be expected if the overload-induced retardation was caused by a crack closure mechanism.

Exactly the same type of behavior has been reported a long time ago by Castro and Parks [35], in a more striking situation. As presented in Fig. 16, after a 200% OL the fatigue crack was arrested, despite the 31% *increase* in ΔK_{eff}. This behavior is again totally incompatible with ΔK_{eff}-controlled FCG.

A final set of experimental results on crack retardation and/or arrest must be discussed. As could be expected

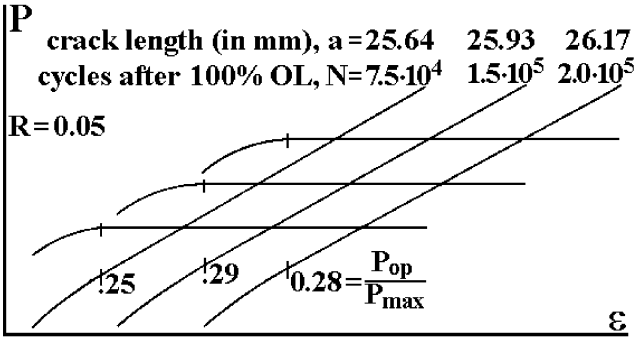

Fig. 15. Crack closure measurements after the 100% OL reported in Fig. 12, made after the crack growth could again be detected. P_{op}/P_{max} progressively *increased* as the crack grew until reaching its previous $P_{op}/P_{max} = 0.28$ value, when the OL effect ceased completely. The various curves have once again been shifted, this time to enhance their differences.

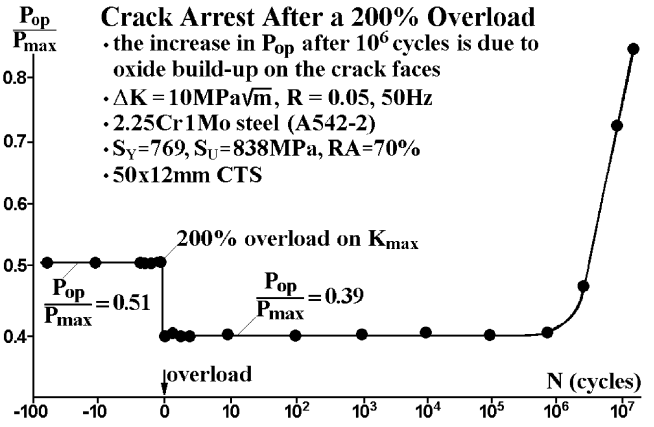

Fig. 16. Crack *arrest* associated with a 31% *increase* in ΔK_{eff}. The OL cycle is arbitrarily called cycle 0, thus cycles before the OL are negative.

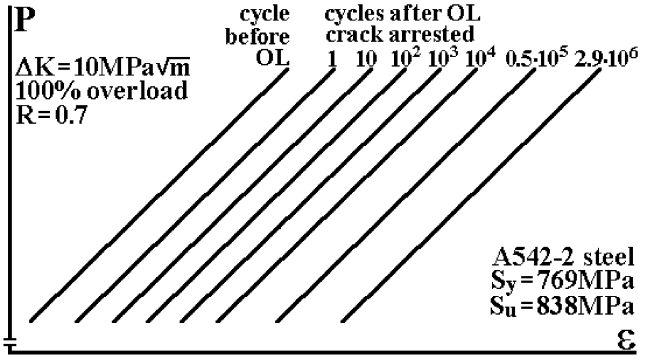

Fig. 17. $P \times \varepsilon$ measurements made before and after a 100% OL that *arrested* the crack when it was growing at a $\Delta K_{BL} = 10$ MPa√m and $R = 0.7$. There is no crack closure before nor after the OL at this high R ratio. The various coincident curves have been shifted for clarity.

from many of the crack closure models discussed above, no crack closure was detected in the $R = 0.7$ FCG tests. Fig. 17 presents some $P \times \varepsilon$ measurements before and after a 100% OL that arrested the crack, when it was growing at a baseline range $\Delta K_{BL} = 10$ MPa√m. Exactly the same behavior was observed in another specimen, this time with a $\Delta K_{BL} = 8$ MPa√m, as shown in Fig. 18.

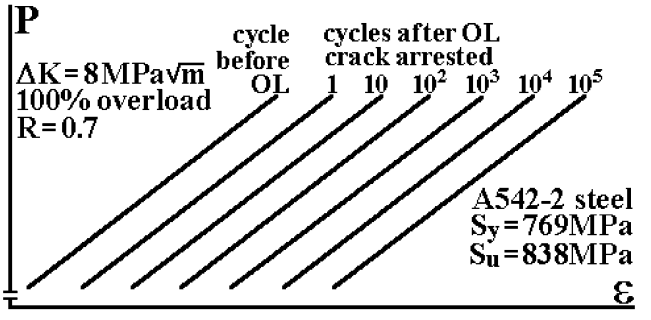

Fig. 18. Other $P \times \varepsilon$ measurements before and after a 100% OL that *arrested* the fatigue crack, this time when it was growing at a $\Delta K_{BL} = 8$ MPa√m and $R = 0.7$. As expected, there is again no detectable crack closure before nor after the OL at this high R ratio, and the various coincident curves have been shifted for clarity.

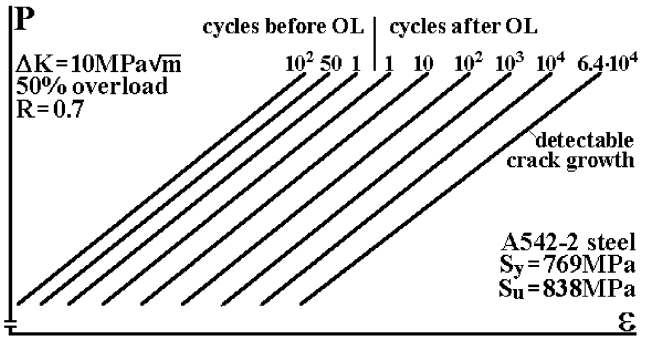

Fig. 19. $P \times \varepsilon$ measurements before and after a 50% OL that *delayed* the crack when it was growing at a ΔK_{BL} = 10 MPa√m and R = 0.7. Once more, there is no crack closure before nor after the overload. The various curves have been shifted, to enhance their differences, particularly the slope change of the $P \times \varepsilon$ curve at $N = 6.4 \times 10^4$ cycles after the OL, when the growth of crack could again be detected.

Also, Fig. 19 presents similar results after a 50% OL which delayed the crack. Since no closure was observed neither before nor after any of these overloads (and, therefore, $\Delta K_{eff} = \Delta K$ during the entire tests), it can be concluded that at these high R ratios crack closure was not a suitable mechanism to explain the observed load cycle interactions in FCG.

4. Conclusion

Fatigue crack closure is the most used mechanism to explain load cycle interactions such as delays in or arrests of the crack growth after overloads. In particular, crack closure has been successfully used to model several OL effects on plane-stress controlled FCG, which has led many researchers to defend the idea that FCG is controlled by ΔK_{eff} and not by ΔK. However, assuming ΔK_{eff} controls all FCG problems could imply in very important thickness effects even under CA loading. Moreover, closure concepts cannot be used to explain some crack delays and arrests measured under plane-strain and under high R ratios. Therefore, it seems that the dominant role of crack closure in the modeling of fatigue crack growth should be reviewed.

References

[1] Paris PC, Tada H, Donald JK. Service load fatigue damage—a historical perspective. Int J Fatigue 1999;21:S35–S46.
[2] Skorupa M. Load interaction effects during fatigue crack growth under variable amplitude loading—a literature review, part 1: Empirical trends. Fatigue Fract Eng Mater Struct 1998;21:987–1006.
[3] Skorupa M. Load interaction effects during fatigue crack growth under variable amplitude loading—a literature review, part 2: Qualitative interpretation. Fatigue Fract Eng Mater Struct 1999;22:905–26.
[4] Sadananda K, Vasudevan AK, Holtz RL, Lee EU. Analysis of overload effects and related phenomena. Int J Fatigue 1999;21:S233–S46.
[5] Lang M, Marci G. The influence of single and multiple overloads on fatigue crack propagation. Fatigue Fract Eng Mater Struct 1999;22:257–71.
[6] Suresh S. Fatigue of materials, 2nd ed. Cambridge, UK: Cambridge University Press; 1998.
[7] Broek D. The practical use of fracture mechanics. Dordrecht, The Netherlands: Kluwer Academic Publishers, 1988.
[8] Elber W. The significance of fatigue crack closure. ASTM STP 486, 1971.
[9] Von Euw EFG, Hertzberg RW, Roberts R. Delay effects in fatigue crack propagation. ASTM STP 513, 1972. p. 230–59.
[10] Newman JCA. Crack opening stress equation for fatigue crack growth. Int J Fract 1984;24(3):R131–R5.
[11] Newman JC, Crews JH, Bigelow CA, Dawicke DS. Variations of a global constraint factor in cracked bodies under tension and bending loads. ASTM STP 1995;1224:21–42.
[12] Castro JTPA. Circuit to measure crack closure. Exp Tech 1993;17(2):23–5.
[13] Ewalds HL, Furnée RT. Crack closure measurements along the crack front in center-cracked specimens. Int J Fract 1978;14:R53–R5.
[14] McEvily AJ. Current aspects of fatigue. Metal Sci 1977;11:274–84.
[15] Paris P.C., Hermann L. Fatigue thresholds, vol. 1. Warley, UK: EMAS; 1982. p. 11–33.
[16] Bernard PJ, Lindley TC, Richards CE. The effect of single overloads on fatigue crack propagation in steels. Metal Sci 1977;11:390–8.
[17] Schijve J. Fatigue of structures and materials. Dordrecht, The Netherlands: Kluwer Academic Publishers, 2001.
[18] Chang JB, Engle RM. Improved damage-tolerance analysis methodology. J Aircraft 1984;21:722–30.
[19] Forman RG, Mettu SR. In: Ernst HA, et al., editors. Behavior of surface and comer cracks subjected to tensile and bending loads in Ti-6AI-4V alloy. ASTM STP 1131, 1992. p. 519–46.
[20] Schijve J. The stress ratio effect on fatigue crack growth in 2024-T3 Alclad and the relation to crack closure. Technische Hogeschool Delft, Memorandum M-336, 1979.
[21] Wang J, Gao JX, Guo WL, Shen YP. Effects of specimen thickness, hardening and crack closure for the plastic strip model. Theor Appl Fract Mech 1998;29:49–57.
[22] Kujawsky D. Enhanced model of partial crack closure for correlation of R-ratio effects in aluminum alloys. Int J Fatigue 2001;23:95–102.
[23] Shih TT, Wei RPA. Study of crack closure in fatigue. Eng Fract Mech 1974;6:19–32.
[24] Führing H, Seeger T. Dugdale crack closure analysis of fatigue cracks under constant amplitude loading. Eng Fract Mech 1979;11(1):99–122.
[25] Bachmann V, Munz D. Fatigue crack closure evaluation with the potential method. Eng Fract Mech 1979;11(1):61–71.
[26] Kim JK, Shim DS. The variation in fatigue crack growth due to the thickness effect. Int J Fatigue 2000;22:611–8.
[27] Park HB, Lee BW. Effect of specimen thickness on fatigue crack growth rate. Nuclear Eng Des 2000;197:197–203.
[28] Costa JDM, Ferreira JAM. Effect of stress ratio and specimen thickness on fatigue crack growth of CK45 steel. Theor Appl Fract Mech 1998;30:65–73.
[29] Mills WJ, Hertzberg RW. The effect of sheet thickness on fatigue crack retardation in 2024-T3 aluminum alloy. Eng Fract Mech 1975;7:705–11.
[30] Saff CR, Holloway DR. In: Roberts R, editor. Evaluation of crack growth gages for service life tracking. Fracture Mechanics, ASTM STP 743, 1981, p. 623–40.
[31] Schijve J. Fundamentals and practical aspects of crack growth

under corrosion fatigue conditions. Proc Inst Mech Engrs 1977;191:107–14.
[32] Shuter DM, Geary W. The influence of specimen thickness on fatigue crack growth retardation following an overload. Int J Fatigue 1995;17(2):111–9.
[33] Shuter DM, Geary W. Some aspects of fatigue crack growth retardation behaviour following tensile overloads in a structural steel. Fatigue Fract Eng Mater Struct 1996;19:185–99.
[34] Suresh S. Micromechanisms of fatigue crack growth retardation following overloads. Eng Fract Mech 1983;18:577–93.
[35] Castro JTP, Parks DM. Decrease in closure and delay of fatigue crack growth in plane strain. Scripta Metall 1982;16:1443–5.
[36] Miranda ACO, Meggiolaro MA, Castro JTP, Martha LF, Bittencourt TN. Fatigue crack propagation under complex loading in arbitrary 2D geometries. In: Braun AA, McKeighan PC, Lohr RD, editors. Applications of Automation Technology in Fatigue and Fracture Testing and Analysis, ASTM STP 1411, 2002. p. 120–46.
[37] Castro JTP. Some critical remarks on the use of potential drop and compliance systems to measure crack growth in fatigue experiments. Brazilian J Mech Sci 1985;7(4):291–314.
[38] Miranda ACO, Meggiolaro MA, Castro JTP, Martha LF. Finite element modeling of fatigue crack bifurcation. In: Bathe KJ, editor. Proc Second MIT Conf on Computational Fluid and Solid Mechanics, Cambridge, MA, USA, 2003. p. 460–3.
[39] Meggiolaro MA, Miranda ACO, Castro JTP, Martha LF. Numerical prediction of the propagation of branched fatigue cracks. In: Bathe KJ, editor. Proc Second MIT Conf on Computational Fluid and Solid Mechanics, Cambridge, MA, USA, 2003. p. 432–5.